The Impact of *In Vivo* Reflectance Confocal Microscopy on the Diagnostic Accuracy of Lentigo Maligna and Equivocal Pigmented and Nonpigmented Macules of the Face

Pascale Guitera[1,7], Giovanni Pellacani[2], Kerry A. Crotty[1], Richard A. Scolyer[3,4], Ling-Xi L. Li[3], Sara Bassoli[2], Marco Vinceti[5], Harold Rabinovitz[6], Caterina Longo[2] and Scott W. Menzies[1,7]

Limited studies have reported the *in vivo* reflectance confocal microscopy (RCM) features of lentigo maligna (LM). A total of 64 RCM features were scored retrospectively and blinded to diagnosis in a consecutive series of RCM sampled, clinically equivocal, macules of the face ($n=81$ LM, $n=203$ benign macules (BMs)). In addition to describing RCM diagnostic features for LM (univariate), an algorithm was developed (LM score) to distinguish LM from BM. This comprised two major features each scoring $+2$ points (nonedged papillae and round large pagetoid cells $>20\,\mu m$), and four minor features; three scored $+1$ point each (three or more atypical cells at the dermoepidermal junction in five $0.5\times0.5\,mm^2$ fields, follicular localization of atypical cells, and nucleated cells within the dermal papillae), and one (negative) feature scored -1 point (a broadened honeycomb pattern). A LM score of $\geqslant2$ resulted in a sensitivity of 85% and specificity of 76% for the diagnosis of LM (odds ratio (OR) for LM 18.6; 95% confidence interval: 9.3–37.1). The algorithm was equally effective in the diagnosis of amelanotic lesions and showed good interobserver reproducibility (87%). In a test set of 29 LMs and 44 BMs, the OR for LM was 60.7 (confidence interval: 11.9–309) (93% sensitivity, 82% specificity).

Journal of Investigative Dermatology (2010) **130,** 2080–2091; doi:10.1038/jid.2010.84; published online 15 April 2010

INTRODUCTION

Lentigo maligna (LM) is a form of melanoma *in situ* that occurs on exposed sun-damaged skin of elderly people with diverse pigmentation types (Ackerman *et al.*, 1993). It remains a frequent diagnostic challenge for clinicians because it often shows overlapping clinical features with benign lesions. As it is often large and located on the face, small biopsy samples are usually collected in an attempt to establish a definite diagnosis before definitive treatment. The condition also presents a challenge for pathologists, particularly in the interpretation of small biopsy specimens. Part of the difficulty in the pathological interpretation of such biopsies occurs because there is often great heterogeneity in the histopathological features of LM in different parts of the lesion. As parts of an LM may display histopathological features of a benign lesion, sampling in small biopsies of areas that do not display typical histopathological features may lead to misdiagnosis (Dalton *et al.*, 2005). Furthermore, in early stages, it may be difficult on histopathology to differentiate LM from melanocytic hyperplasia in sun-damaged skin (Klauder and Beerman, 1955; Cohen, 1996; Weyers *et al.*, 1996). LM also represents a therapeutic challenge because of its usual size as well as location and propensity to locally recur, estimated to be between 8 and 31% after conventional surgery (Agarwal-Antal *et al.*, 2002; Osborne and Hutchinson, 2002; McKenna *et al.*, 2006). Furthermore, determination of the peripheral margins of LM clinically and pathologically also represents another challenge. Clinically, LM is often amelanotic peripherally, and can spread far beyond the visible margins (McKenna *et al.*, 2006). Dermoscopy (Schiffner *et al.*, 2000; Robinson, 2004; Stante *et al.*, 2005) and Wood's light examination (Jeneby *et al.*, 2001) have been described as useful techniques to

[1]*Sydney Melanoma Diagnostic Centre and Dermatology Department, Royal Prince Alfred Hospital, Camperdown, New South Wales, Australia;* [2]*Department of Dermatology, University of Modena and Reggio Emilia, Modena, Italy;* [3]*Department of Anatomical Pathology, Royal Prince Alfred Hospital, University of Sydney, Sydney, New South Wales, Australia;* [4]*Discipline of Pathology, Faculty of Medicine, University of Sydney, Sydney, New South Wales, Australia;* [5]*Department of Hygiene and Public Health, University of Modena and Reggio Emilia, Modena, Italy;* [6]*Skin and Cancer Associates, Plantation, Florida, USA and* [7]*Discipline of Dermatology, Sydney Medical School, University of Sydney, Sydney, New South Wales, Australia*

Correspondence: Scott W. Menzies, Department of Dermatology, University of Sydney, Sydney Melanoma Diagnostic Centre, Sydney Cancer Centre, Royal Prince Alfred Hospital, Camperdown, New South Wales 2050, Australia. E-mail: scott.menzies@sswahs.nsw.gov.au

Abbreviations: BM, benign macule; LM, lentigo maligna; OR, odds ratio; RCM, reflectance confocal microscopy

Received 20 November 2008; revised 29 September 2009; accepted 24 December 2009; published online 15 April 2010

better define the extent of the lesion. Mohs' surgery (Zitelli *et al.*, 1991; Bricca *et al.*, 2005; Bhardwaj *et al.*, 2006; Bene *et al.*, 2008), staged excision (Bub *et al.*, 2004; Huilgol *et al.*, 2004; Mahoney *et al.*, 2005; Hazan *et al.*, 2008), and three-dimensional histology (Moehrle *et al.*, 2006) have been proposed as techniques to more precisely delineate the margins of LM but are expensive and the procedures require a high degree of expertise (Barlow *et al.*, 2002, 2007).

In vivo reflectance confocal microscopy (RCM) provides a cellular resolution in the upper layers of the skin and has been shown to improve melanoma diagnostic accuracy (Pellacani *et al.*, 2007; Guitera *et al.*, 2009). As melanin/melanosomes appear bright under reflectance at near-infrared wavelengths, pigmented cells are easily visualized and RCM features can be evaluated for diagnosis (Rajadhyaksha *et al.*, 1995). Furthermore, as RCM generates a horizontal view (of at least $4 \times 4\,mm^2$), it is possible to assess more of the lesion using this technique than with pathological assessment of vertically orientated small biopsy specimens (even with step sectioning) that are usually examined in routine histopathology (Guitera *et al.*, 2009).

Preliminary reports show that RCM can be used to differentiate LM from other pigmentations of the face (Tannous *et al.*, 2002; Langley *et al.*, 2006) and can assist in defining peripheral margins of LM (Chen *et al.*, 2005), even amelanotic tumors (Curiel-Lewandrowski *et al.*, 2004).

The aims of this study were to define which RCM features can distinguish LM from benign macules (BMs) of the face such as solar lentigo, ephelis, actinic keratosis, and flat seborrheic keratosis, and to test different algorithms for diagnosing LM (a method published previously and a new algorithm).

RESULTS

Study population

The study population comprised a total of 219 patients. Lesions from 146 patients, corresponding to 76 women and 70 men (mean age of 62 years, 25–75% percentiles: 51–72 years) were retrieved from the digital archives of the University of Sydney and of the University of Modena and used as the training set. In addition, 73 cases from as many patients collected in Sydney (Australia), Modena (Italy), and Plantation (FL, USA), constituted the test set.

In the training set, there were 61 LM patients, 27 women and 34 men (mean age of 66 years, 25–75% percentiles: 56–75). Multiple biopsy samples (a total of 138) were collected from different regions of 39 lesions, in an attempt to obtain an accurate presurgical diagnosis or to delineate the margins of ill-defined tumors. Overall, 25 of these 39 lesions were LMs, whereas the remaining 14 were BMs (mostly actinic keratoses and solar lentigos that on previous biopsies were not diagnostic). Therefore, the LM group included a total of 81 LM biopsy-proven areas with matching RCM images, comprising 61 biopsies from within the lesions themselves and 20 further perilesional biopsies collected for peripheral margin determination. The 203 BMs of the face (obtained from 85 cases and 118 sites from the margins of 25 LMs and 14 BMs) included 116 showing solar-damaged skin (solar elastosis, melanocytic hyperplasia), 25 actinic keratoses, 21 solar lentigos, 21 pigment incontinence or lichen planus-like keratoses, 8 seborrheic keratoses, 7 ephelitides, and 5 junctional nevi. The study population excluded all nonbiopsied lesions, LM melanomas, Bowen's disease, flat basal cell carcinomas, and all histopathologically equivocal ''borderline'' or ''early'' LM lesions. However, this latter nonstudy group was analyzed prospectively following development of algorithms.

Significant features

All RCM features scored are reported in Table 1.

Superficial layer features. As in other types of melanoma, the presence of marked epidermal disarray (Pellacani *et al.*, 2007) was more frequently observed in LMs (56%), although it was also present in 18% of BMs of the face. A homogeneous epidermis, characterized by a regular honeycombed pattern, was strongly correlated with BM (92%). It is noteworthy that a broadened honeycomb (Figure 1) was more frequently observed in BMs of the face (16%)—and in particular, in actinic keratoses and seborrheic keratoses (10 out of 33) with an odds ratio (OR) of 0.3 for LM. In contrast, the atypical cobblestone pattern, particularly when composed of small nucleated cells (Figure 2), was strongly associated with LM (OR of 13.3) but was uncommon (6% of LM).

A new descriptor of epidermal thickness (evaluated at the center of the lesion to be $<25\,\mu m$ from under the stratum corneum to the beginning of the dermoepidermal junction in the region of suprapapillary plates) was more frequent in LM (21%) compared with BM (12%), but with a lower OR of 2.

Pagetoid infiltration was reported in 75% of LMs and 28% of BMs of the face (OR of 7.8). In particular, when it was constituted by round and large ($>20\,\mu m$) cells, the OR was higher at 10.3 (Figure 3), whereas the observation of dendritic pagetoid cells had a relatively lower OR of 6.1. The characteristic of the dendritic pagetoid cells, being either small or large, with thin or thick dendrites, with arborizing or retiform dendrites, made no major difference, with ORs of between 3 and 5 for all these categories. When the pagetoid cells were widespread, pleomorphic, in clusters of three, or numerous (three or more pagetoid cells found on five images of $0.5 \times 0.5\,mm^2$), they were strongly associated with LM, with ORs >7.

At the dermoepidermal junction level. Nonedged papillae (dermal papillae without a demarcated rim of bright cells, but separated by a series of large reflecting cells) were observed in 68% of LMs and in 17% of BMs of the face (OR of 10.5) (Figure 4), whereas mild and/or marked atypia was observed in 89 and 37%, respectively (OR of 13.7). More than three atypical cells at the junction in five images (field of view $0.5 \times 0.5\,mm^2$) was one of the most significant criteria for LM diagnosis (OR of 13.8), and was present in 86% of LMs (Figure 5). Interestingly, clusters (nests) and thickening at the dermoepidermal junction were also predominant in LMs (OR of 6.3 and 4.9, respectively), even if present in $<15\%$ of LMs. A thin dark featureless area around a few or one atypical cell

Table 1. RCM features discriminating lentigo malignas (LMs) and benign macules (BMs) of the face

RCM feature	% Agreement	81 LMs (%)	203 BMs (%)	OR (CI95%) when significant or *P*-value when nonsignificant	Standardized discriminant analysis coefficient	Binary logistic regression coefficient
Upper layers						
Thick stratum corneum		0	9 (4.4)	*P*=0.06		
Parakeratosis, defined as dark roundish structures within keratinocytes with large cytoplasm		1 (1.2)	5 (2.5)	*P*=0.68		
Milia cyst >10 on $4 \times 4\,mm^2$, defined as round, homogenously refractive nodule, 30–50 μ diameter		0	1 (0.5)	*P*=1		
Regular honeycombed pattern		60 (74.1)	188 (92.6)	0.2 (0.1–0.5)		
Epidermal disarray		46 (56.8)	36 (73)	6.1(3.5–10.7)		
Thin epidermis (<25 μm)		17 (20.9)	24 (11.8)	2 (1–3.9)		
Atypical honeycombed		17 (21)	59 (29.1)	*P*=0.17		
Broadened honeycombed	91.5	4 (4.9)	32 (15.7)	0.3 (0.1–0.8)	−0.85	−1.990
Polarized honeycomb pattern defined as polarized elongated mesh-like structures.		1 (1.2)	2 (1)	*P*=1		
Diamond shape honeycomb pattern with irregular diamond-shaped large cells (>20 μ).		1 (1.2)	7 (3.4)	*P*=0.45		
Fibrillar polarized pattern, as fibrillary polarized cells drawing a reticulation pattern and disrupting the normal epidermis structure, described in basal cell carcinoma (Nori *et al.*, 2004).		2 (2.5)	1 (0.5)	*P*=0.20		
Dark shadow, as large dark featureless area with blurred border disrupting the normal epidermis described as clefting in basal cell carcinoma (Agero *et al.*, 2006).		0	3 (1.5)	*P*=0.56		
Cobblestone pattern		11 (13.6)	15 (7.4)	*P*=0.10		
Atypical cobblestone pattern		7 (8.6)	3 (1.48)	6.3 (1.6–25)		
Atypical cobblestone with small nucleated cells		5 (6.1)	1 (0.5)	13.3 (1.5–115.6)		
Grainy image		33 (47)	38 (19.7)	3 (1.7–5.3)		
Pagetoid cells		61 (75.3)	57 (28.1)	7.8 (4.3–14.1)		
Round pagetoid cells		47 (58.1)	36 (17.7)	6.4 (3.6–11.3)		
Round pagetoid cells >20 μ	85.7	30 (37.0)	11 (5.4)	10.3 (4.8–21.9)	1.096	1.411
Round pagetoid cells <20 μ		22 (27.2)	27 (13.3)	2.4 (1.3–4.589)		
Round pagetoid cells with halo		24 (29.6)	19 (9.4)	4.1 (2.1–8)		
Dendritic pagetoid cells		44 (54.3)	33 (16.3)	6.1 (3.4–10.9)		
Dendritic pagetoid cells >20 μ		20 (24.7)	17 (8.4)	3.6 (1.8–7.3)		
Dendritic pagetoid cells <20 μ		27 (33.3)	21 (10.3)	4.3 (2.3–8.3)		
Dendritic pagetoid cells with thin dendrites		33 (40.7)	27 (13.3)	4.5 (2.5–8.2)		
Dendritic pagetoid cells with thick dendrites		16 (19.7)	15 (7.4)	3.1 (1.4–6.6)		
Dendritic pagetoid cells with 1 or 2 dendrites		17 (20.9)	14 (6.9)	3.6 (1.7–7.7)		
Dendritic pagetoid cells with arborizing dendrites		21 (25.9)	19 (9.4)	3.4 (1.7–6.7)		
Retiform dendrites without ovoid body visible		25 (30.9)	20 (9.9)	4.1 (2.1–7.9)		
Widespread pagetoid infiltration		29 (35.8)	13 (6.4)	8.2 (4–16.8)		
Pleomorphic pagetoid infiltration		29 (35.8)	14 (6.9)	7.5 (3.7–15.3)		
Follicular localization of pagetoid cells		21 (25.5)	15 (7.4)	4.4 (2.1–9)		
More than three Pagetoid cells in a cluster		12 (14.8)	4 (1.9)	8.7 (2.7–27.7)		
More than three Pagetoid cells in five ($0.5 \times 0.5\,mm^2$) images		56 (69.1)	46 (22.7)	7.6 (4.3–13.6)		
Pagetoid cells round and large and/or dendritic and small		47 (58)	29 (14.3)	8.3 (4.6–15)		

Table 1 continued on the following page

Table 1. Continued

RCM feature	% Agreement	81 LMs (%)	203 BMs (%)	OR (CI95%) when significant or *P*-value when nonsignificant	Standardized discriminant analysis coefficient	Binary logistic regression coefficient
Dermal epidermal junction						
Edged papillae		25 (31)	77 (25)	*P*=0.26		
Nonedged papillae	75.8	55 (67.9)	34 (16.7)	10.5 (5.8–19.1)	1.229	1.602
Nonvisible papillae		10 (12.3)	91 (44.8)	0.2 (0.1–0.4)		
Polycyclic papillae, as circumvolution of edged papillae described in solar lentigines (Langley *et al.*, 2006)		12 (14.8)	34 (16.8)	*P*=0.69		
Nonatypical cells at the junction		1 (1.2)	2 (1)	*P*=1		
Mild and marked cellular atypia		72 (88.9)	75 (36.9)	13.7 (6.5–28.9)		
More than three atypical cells in a total of five $0.5 \times 0.5\,mm^2$ images	82.9	70 (86.4)	64 (31.5)	13.8 (6.9–27.9)	0.690	1.254
Mild pleomorphism		39 (48.1)	54 (26.6)	2.6 (1.5–4.4)		
Marked pleomorphism		31 (38.3)	15 (7.4)	7.8 (3.9–15.5)		
Atypical cells with dark halo		23 (28.4)	17 (8.4)	4.3 (2.2–8.7)		
More than three atypical cells in a cluster		29 (35.8)	18 (8.9)	5.7 (3–11.1)		
Atypical cells around the follicular extension		38 (46.9)	25 (12.3)	6.3 (3.4–11.5)		
Follicular extension of pagetoid cells and/or atypical junctional cells	80.0	48 (59.3)	32 (15.8)	7.8 (4.3–13.9)	0.667	0.950
Sheet of cells		7 (8.7)	3 (1.5)	6.3 (1.6–25)		
Junctional clusters		7 (8.7)	3 (1.5)	6.3 (1.6–25)		
Junctional thickenings		12 (14.8)	7 (3.4)	4.9 (1.89–12.9)		
Upper dermis						
Nests		7 (8.6)	4 (1.9)	4.7 (1.3–16.5)		
Dense nest		3 (3.7)	2 (1)	*P*=0.14		
Dishomogeneous nest		4 (4.9)	2 (1)	*P*=0.06		
Nucleated cells within the papilla	92.8	12 (14.8)	4 (1.9)	8.7 (2.7–27.7)	0.929	
Plump bright cells		34 (41.9)	44 (21.7)	2.6 (1.5–4.5)		
Plump bright cells sparse within the papillary dermis		16 (19.7)	9 (4.4)	5.3 (2.2–12.6)		
Plump bright cells confluent		17 (20.1)	34 (16.7)	*P*=0.4		
Plump bright cells in big aggregation within the papillary dermis		10 (12.3)	15 (7.4)	*P*=0.18		
Bright small cells and/or hyperreflecting spots		30 (37)	46 (22.7)	2 (1.1–3.5)		
Broadened reticulated collagen fibers		34 (41.9)	117 (57.6)	0.5 (0.3–0.9)		
Collagen bundles		11 (13.6)	10 (4.9)	3 (1.2–7.5)		
Thin collagen fibers		5 (6.2)	17 (8.37)	*P*=0.53		
Curled highly refractive collagen fibers		7 (8.6)	18 (8.9)	*P*=0.95		
Nonvisible vessels		68 (83.9)	169 (83.2)	*P*=0.89		
RCM score $\geqslant 3$		64 (79.0)	46 (22.7)	12.8 (6.9–24.1)		
LM score $\geqslant 2$	87.2	69 (85.2)	48 (23.6)	18.6 (9.3–37.1)		

Abbreviations: CI95%, 95% confidence interval; OR, odds ratio; RCM, reflectance confocal microscopy.

(dark halo) in the epidermis (round pagetoid cells) or at the dermoepidermal junction was a new descriptor (Figure 6) that was useful for the diagnosis of LM, and was seen in <10% of BMs of the face (OR of 4.1 and 4.3, respectively). Similarly, follicular localization of atypical cells (Figure 7) in the epidermis and/or at the junction level was seen in <16% of BMs of the face (OR for the diagnosis of LM of 7.8).

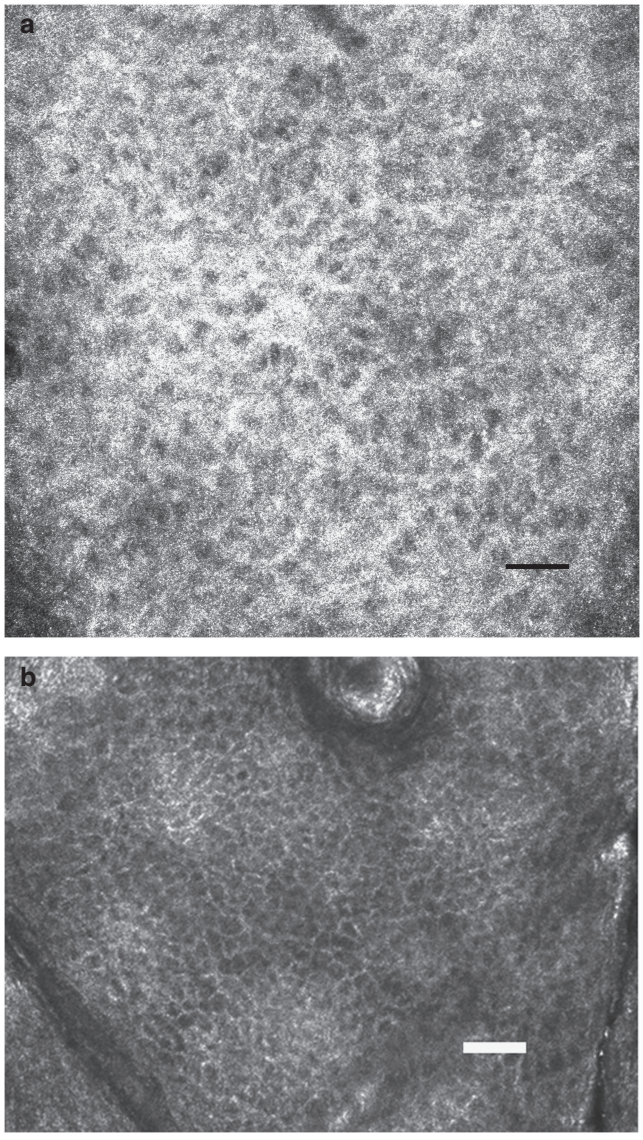

Figure 1. Different types of honeycomb pattern. (**a**) *In vivo* confocal microscopy image of a broadened honeycomb pattern in the epidermis of a macular seborrheic keratosis of the scalp. (**b**) *In vivo* confocal microscopy image of a normal honeycomb pattern in the epidermis (bar = 50 μm).

In the papillary dermis. Overall, 15% of the LMs showed large nucleated cells within the dermal papillae, compared with 2% of BMs of the face, giving this criteria an OR of 8.7 for the diagnosis of LM (Figure 8). Dermal nests were very rare (7 out of 81 LMs) and more associated with LM (OR of 4.7). They were dishomogeneous in four cases and dense in three cases. Plump bright cells, particularly sparse within the papillary dermis, were strongly associated with the LMs (OR of 5.3). Broadened reticulated collagen fibers were mostly associated with BMs of the face (58%), whereas collagen bundles were mostly associated with LM but were present in only 14% of biopsies.

The features that were not significantly different between LMs and BMs of the face are listed in Table 1, with their definitions.

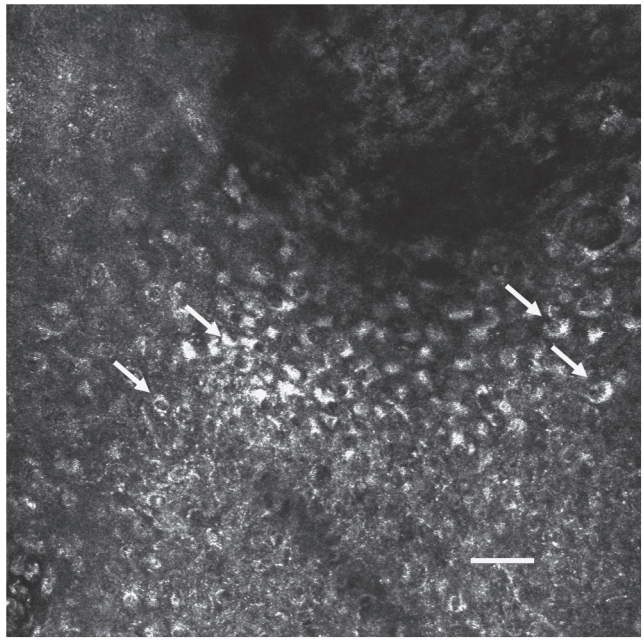

Figure 2. Atypical cobblestone pattern. *In vivo* confocal microscopy image of an atypical cobblestone pattern with small bright nucleated cells of the epidermis of a lentigo maligna (LM) of the R cheek (bar = 50 μm).

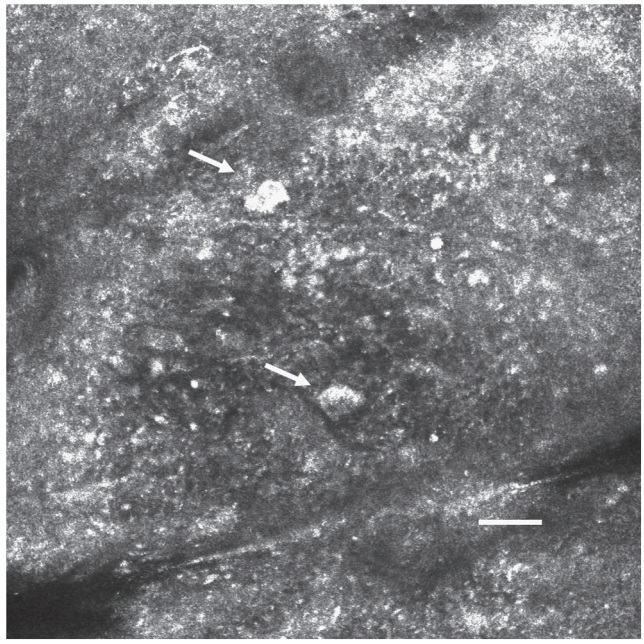

Figure 3. Large pagetoid cells. *In vivo* confocal microscopy image of large pagetoid cells (arrows) in the upper layer of the epidermis of a lentigo maligna melanoma (LMM) (0.2 mm Breslow thickness). Bar = 50 μm.

LM score. Analysis of the study population showed that six features were independently correlated with malignancy by means of discriminant analysis, corresponding to, in order of relevance:

- nonedged papillae,
- pagetoid round and large cells,
- nucleated cells in a dermal papilla,

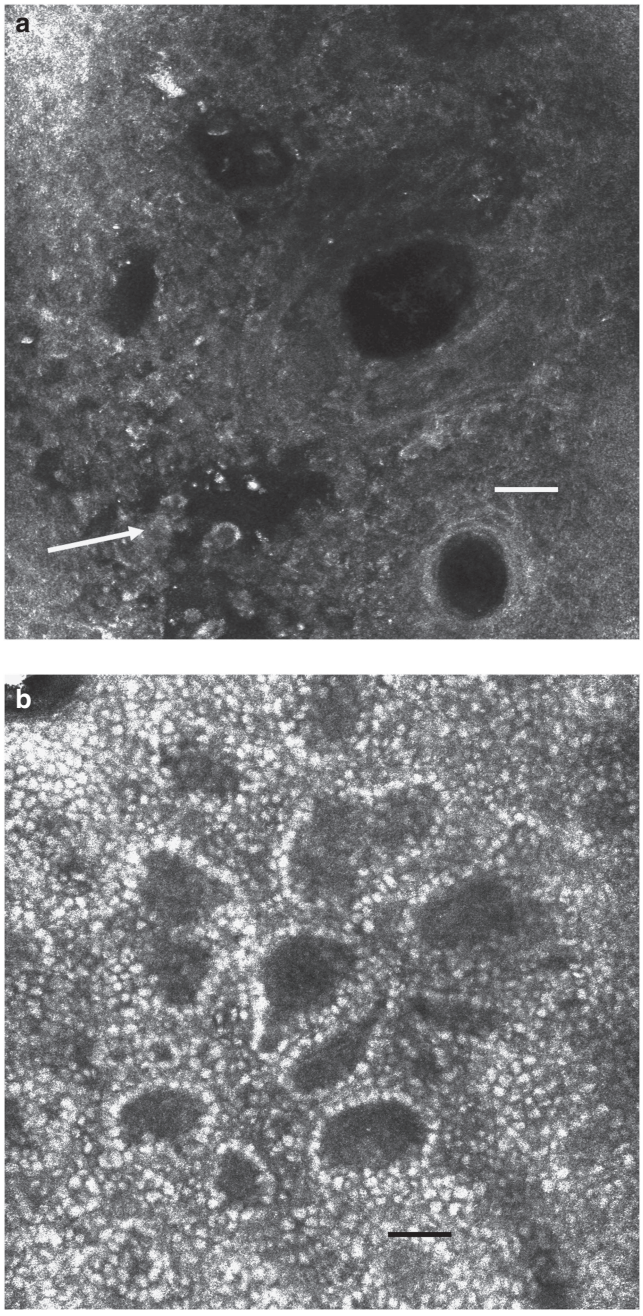

Figure 4. Nonedge and edge papillae. (**a**) *In vivo* confocal microscopy image of nonedge papillae and atypical cells at the dermoepidermal junction (arrows) of a lentigo maligna (LM) of the cheek. (**b**) *In vivo* confocal microscopy image of edge papillae of a benign (clinically and dermoscopically) pigmented macule of the face not biopsied (nonstudy example) (bar = 50 μm).

- three or more atypical cells at the dermoepidermal junction in five $0.5 \times 0.5\ mm^2$ images,
- follicular localization of pagetoid cells and/or atypical junctional cells, and
- the single negative (benign) feature of broadened honeycomb pattern of the epidermis.

Binary logistic regression confirmed that all but nucleated cells in the dermis were significant (Table 1).

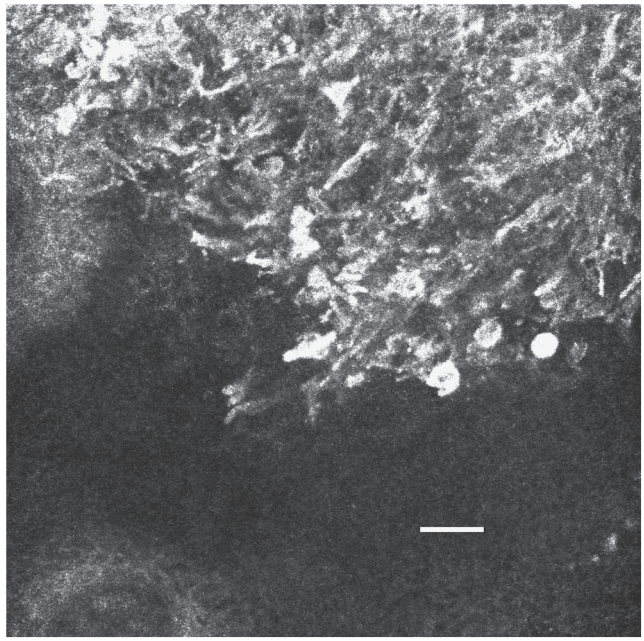

Figure 5. Atypical cells. *In vivo* confocal microscopy image of numerous atypical cells (both dendritic and large roundish cells) at the dermoepidermal junction of a lentigo maligna (LM) of the L cheek (bar = 50 μm).

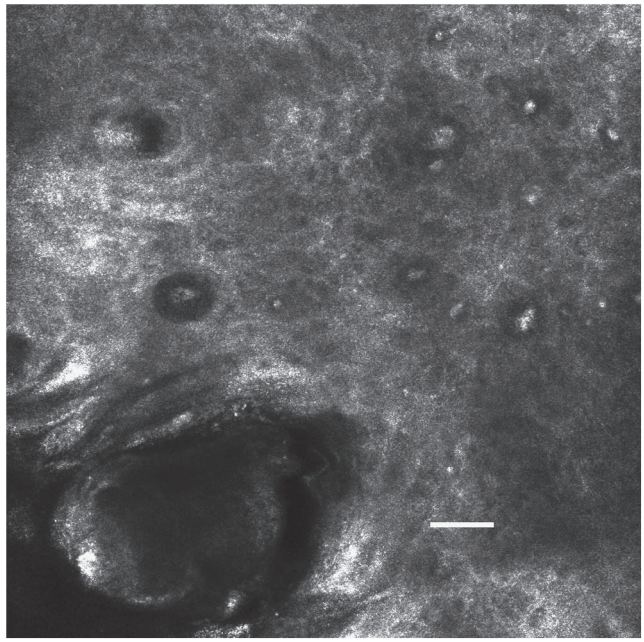

Figure 6. *In vivo* confocal microscopy image of a black halo around atypical cells in the epidermis of a lentigo maligna (LM) of the cheek. Examination of the sections showed no obvious histopathological correlation for these halo cells (bar = 50 μm).

According to discriminant analysis and binary logistic regression weight of the features (see Table 1), a simplified algorithm was developed (Table 2), termed ''LM score,'' which evaluated the presence of two major features that scored 2 points each (nonedged papillae and round pagetoid

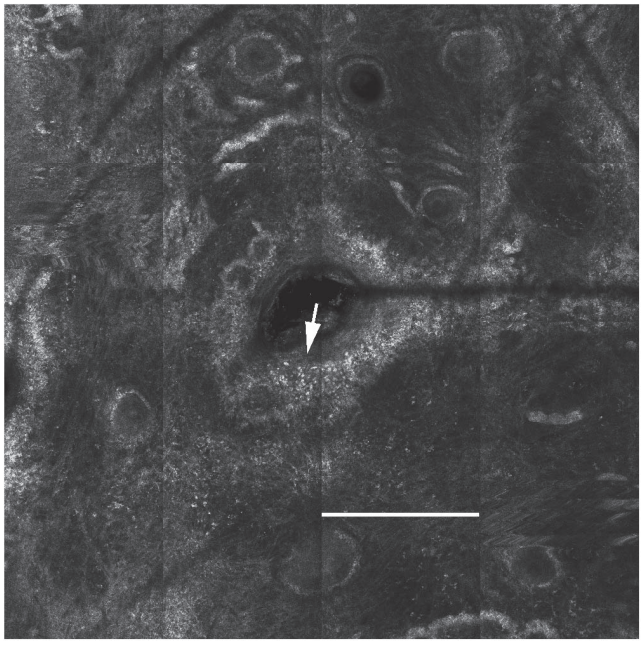

Figure 7. Follicular localization of atypical cells. Reconstruction of a horizontal plan of 2 mm with 16 *in vivo* confocal microscopy images (bar = 0.5 mm) of a follicular localization of atypical cells (arrow) at the dermoepidermal junction of a lentigo maligna (LM) of the scalp.

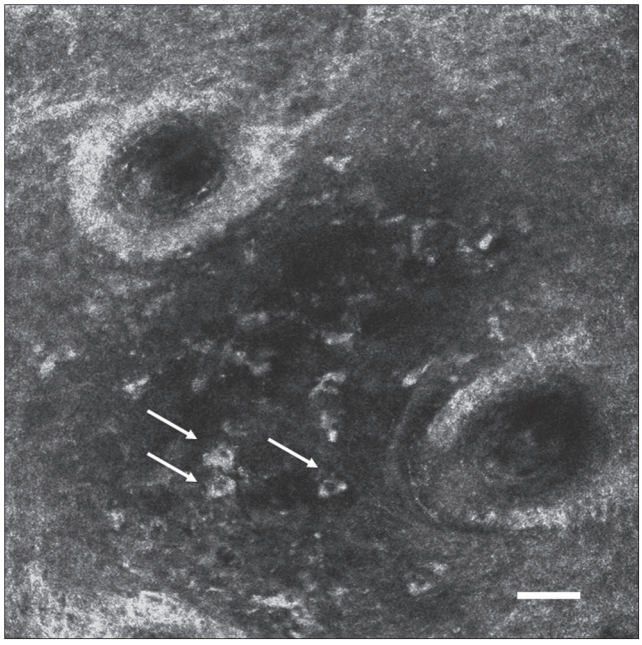

Figure 8. Nucleated cells in the dermis. *In vivo* confocal microscopy image of single nonnested large nucleated cells that were considered to be in the papillary dermis (arrows), of a lentigo maligna (LM) of the cheek (bar = 50 μm).

cells >20 μm), and four minor features; three positive features scored one point each (three or more atypical cells at the junction in five images, follicular localization of pagetoid cells, and/or atypical junctional cells, nucleated cells within the dermal papillae), and one negative feature, scored minus 1 point (broadened honeycomb pattern). This new LM score algorithm produced a sensitivity of 93% and a specificity of 61% for a score ⩾1. However, the threshold of ⩾2 produced the highest diagnostic accuracy with a sensitivity of 85% and a specificity of 76% (OR 18.6 (95% confidence interval: 9.3–37.1).

The percentage of agreements between the two RCM experts on the most significant features are reported in Table 1. The overall agreement on the LM score was 87.2% ($\kappa = 0.740$).

Details of the subgroups of the study population with LM score ⩾2 are provided in Table 3. There was no significant difference in the sensitivity of the LM score for diagnosis of cases ($n = 61$) or margin determination ($n = 20$) ($P = 0.49$). Out of the 20 pathologically LM-proven peripheral margin sites, 9 were completely amelanotic and 100% of these 9 had an LM score ⩾2. The LM score had a specificity for the five junctional nevi of 60% and had a similar specificity for all types of keratoses: 62.5% for seborrheic keratoses ($n = 8$), 64% for actinic keratoses ($n = 25$), and 67% for lichen planus-like keratoses and pigment incontinence ($n = 21$). It had a higher specificity for solar lentigo (76%) and sun-damaged skin with solar elastosis and melanocytic hyperplasia found primarily in samples for determining LM margins (83%).

Interestingly, the specificity of the LM score was higher when the BMs of the face were amelanotic (90%, $n = 67$), or lightly pigmented (87%, $n = 53$) compared with partially or darkly pigmented cases (59%, $n = 83$) ($P < 0.001$). The sensitivity of the method varied, with 93% for amelanotic LM ($n = 14$), 78% for the light-colored lesions ($n = 9$), and 84% for the partially or darkly pigmented lesions ($n = 49$).

Test set. We compared the previously reported RCM score (Table 2; Pellacani *et al.*, 2007) for the diagnosis of melanoma (non-LM subtype) with the newly developed LM score on an independent test set of 73 cases (29 LMs and 44 BMs). Both LM and RCM scores showed a sensitivity of 93 and 83%, respectively, and a specificity of 82 and 86%, respectively. The OR for the diagnosis of LM was 60.8 (11.9–309) and 30.4 (8.3–110.7), respectively, but failed to reach significant difference ($P = 0.114$).

The LM score was also tested on other groups of patients (not included in the study group) and showed a similar sensitivity (83%) for six invasive LM melanomas (median Breslow thickness 0.34 mm). In contrast, it showed a poor sensitivity on LM that was classified as uncertain or ''early'' LM by pathology (22%). The BM of the face that was digitally monitored and had not changed for more than 12 months were classified as benign in 91% of cases ($n = 30$). The epithelial tumors (13 macular basal cell carcinomas and 2 Bowen's disease) were also correctly classified as non-LM in 93% of cases.

DISCUSSION

We studied a large series of 110 LMs and 247 BMs of the face assessed with *in vivo* RCM, confirming preliminary case reports showing that RCM can be used to differentiate LM

Table 2. Simplified *in vivo* confocal methods for the diagnosis of LM (LM score) and other types of melanoma (RCM method, Pellacani *et al.*, 2007)

RCM score	LM score
Two major features, each scored 2 points	*Two major features, each scored 2 points*
Nonedged papillae	Nonedged papillae
Cellular atypia at dermal–epidermal junction	Pagetoid cells round and >20 μm
Four minor features, each scored 1 point	*Three minor features, each scored 1 point*
Roundish pagetoid cells	More than three atypical cells at the junction in five images
Widespread pagetoid infiltration	Follicular localization of pagetoid cells and/or atypical junctional cells
Cerebriform nests	Nucleated cells within the papilla
Nucleated cells within the papilla	
	One minor negative feature, score −1 point—broadened honeycomb pattern

Abbreviations: LM, lentigo maligna; RCM, reflectance confocal microscopy.

Table 3. Performance of the LM score ⩾2 on subgroups of the study population and initially excluded cases

	LM score <2, *N* (%:CI95%)	LM score ⩾2, *N* (%:CI95%)	Total
LM (total)	12 (14.8: 7.1–22.5)	69 (85.2: 77.2–92.8)	81
LM cases	10 (16.4: 7.1–25.7)	51 (83.6: 74.3–92.9)	61
LM margins	2 (10: 0–23.1)	18 (90: 76.8–100)	20
BM of the face (total)	155 (76.4: 70.5–82.2)	48 (23.7: 17.8–29.5)	203
Solar elastosis, melanocytic hyperplasia	96 (82.8: 75.9–89.6)	20 (17.2: 10.4–24.1)	116
Actinic keratoses	16 (64: 45.2–82.8)	9 (36: 17.2–54.8)	25
Pigment incontinence, inflammation, LPLK	14 (66.7: 46.5–86.8)	7 (33.3: 13.2–53.5)	21
Solar lentigo	16 (76.2: 57.9–94.4)	5 (23.8: 5.6–42)	21
Seborrheic keratoses	5 (62.5: 28.9–96)	3(37.5: 3.9–71)	8
Ephelis	5 (71.4: 38–100)	2 (28.6: 0–62)	7
Junctional nevus	3 (60: 17.1–100)	2 (40: 0–82.9)	5
LM score for other groups (excluded)			
Epithelial tumors total	14 (93.3: 80.7–100)	1 (6.7: 0–19.3)	15
BCC	12 (92.3: 77.8–100)	1 (7.7: 0–22.2)	13
Bowen's	2 (100: NA)	0	2
Long digital follow-up (>12 months) unchanged	27 (90: 79.3–100)	3 (10: 0–20.7)	30
Histologically equivocal LM	7 (77.8: 50.6–100)	2 (22.2: 0–49.4)	9
Invasive LM melanoma	1(16.7:0–46.5)	5 (83.3: 53.5–100)	6

Abbreviations: BCC, basal cell carcinoma; BM, benign macule; CI95%, 95% confidence interval; LM, lentigo maligna; LPLK, lichen planus-like keratoses; NA, nonapplicable.

from other pigmentations of the face (Langley *et al.*, 2006) and assist in defining LM peripheral margins (Chen *et al.*, 2005), even in amelanotic lesions (Curiel-Lewandrowski *et al.*, 2004).

Furthermore, we showed that six features were independently correlated with malignancy by means of discriminant analysis, and five with logistic regression analysis, allowing us to build a simplified RCM diagnostic algorithm. The LM score comprising only six features was highly reproducible as demonstrated by an 87% agreement between two observers. The features corresponded to, in order of relevance:

- *Nonedged papillae*: This criterion is also a major criterion in the previously published RCM melanoma score

(Pellacani *et al.*, 2007), developed on other types of melanomas and corresponds to distortion of the dermoepidermal junction by atypical cells.

- *Round and large pagetoid cells*: Both widespread pagetoid cells and round pagetoid cells are minor criteria in the previously published RCM score. The fact that size is an important feature for the diagnosis of LM may be due to the reason that numerous BMs of the face show some melanocytic hyperplasia and/or hyperpigmented keratinocytes that may be interpreted under confocal microscopy as small pagetoid cells. A threshold of 20 μm appears to aid in distinguishing them from malignant melanocytes.
- *Three or more atypical cells at the junction in five images*: Finding atypical cells at the junction is also a major criterion in the RCM score. In LM, they had to be numerous ($\geqslant 3$) to be discriminant. Again, the fact that numerous BMs of the face contain some melanocytic hyperplasia may explain the necessity of more stringent criteria to differentiate LM from BM of the face.
- *Follicular localization of pagetoid cells and/or atypical junctional cells*: This criterion is specific to the LM type of melanoma under RCM, as it was not found by the previous RCM method algorithm on other melanoma subtypes (Pellacani *et al.*, 2007). It correlates with the histopathological findings (Ferrara *et al.*, 2008) and also the dermoscopy findings of asymmetric pigmented follicular openings (Schiffner *et al.*, 2000).
- *Nucleated cells in the dermal papillae*: Although this is a minor criterion in the previous RCM score, it is surprising that it is important in the diagnosis of LM (which is by definition confined to the epidermis). The reason for the apparent discrepancy between the RCM and pathology findings may be related to sampling such that the dermal component identified on RCM was not present in the pathology biopsy sections. Alternatively, difficulty in determining the exact site of the cells (junctional or dermal) on RCM is another possible explanation, especially as the dermoepidermal junction was partially disrupted in many cases. The same explanation may apply to the very few ''dermal'' nests that have been found in LM cases by confocal microscopy in our study, but were not identified in histopathological examination of the biopsy specimens. Future research should evaluate the role of *in vivo* RCM in detecting early dermal invasion in LM melanoma.
- *Broadened honeycomb pattern of the epidermis*: This negative criterion is a new feature and seemed to be specific for benign keratoses.

Some other pathology components of classical LM such as thin epidermis, solar elastosis (corresponding to collagen bundles), and melanophages (corresponding to plump bright cells) were also found to be more closely associated with LM, but were less significant than the aforementioned criteria.

The threshold of $\geqslant 2$ for the LM score had a sensitivity of 93% and a specificity of 82% for the diagnosis of LM with an OR = 60.8 for LM as achieved in the test set. Although the diagnostic accuracy of the LM score (as expressed by the OR) was superior to the previously described RCM method used for melanoma of the non-LM subtype (Pellacani *et al.*, 2007), this improvement failed to reach statistical significance. It is noteworthy that the improved sensitivity and specificity found in the test set may be due to the incorporation of additional cases by the Florida group, not found in the training set.

It is well known that the distinction between LM and BM are often very difficult clinically and also pathologically, particularly in small biopsy specimens of heavily sun-damaged skin. Targeting punch biopsies to the middle of the confocal field seemed to afford better histological–confocal correlation in LM, which often contains irregular margins of scattered cells. The LM score performed as well on peripheral LM margins ($n = 20$) as on biopsies from the lesions themselves ($n = 61$) in the training set, even though the peripheral sites were often completely amelanotic (9 out of 20). It was previously described that the diagnostic accuracy of the RCM method was significantly superior for amelanotic and light-colored lesions compared with partially and completely pigmented lesions (Guitera *et al.*, 2009). This may be explained by the fact that melanin appears very bright under reflectance microscopy, even if it is only present in very small quantities (Rajadhyaksha *et al.*, 1995). Indeed, immunohistochemical and ultrastructural studies show that amelanotic melanoma cells contained melanosomes and rare melanin granules even if they are not visible clinically (Erlandson, 1987; Gibson and Goellner, 1988).

It is noteworthy that keratoses were less easy to differentiate from LMs than other BMs of the face, perhaps due to the distortion of pigmented keratinocytes that had a similar reflectance signal under RCM to atypical melanocytes. In this series, junctional nevi were often classified as LM by RCM. However, even though there were few cases ($n = 5$), all these cases were considered ''dysplastic'' with some mild atypia. It has been suggested that such lesions may represent a precursor to LM in some patients (Kossard *et al.*, 1991).

The prospective use of the LM score on a different study set also validated our findings with a similar sensitivity (83%) for thin LM melanomas (0.34 mm Breslow thickness) and higher specificity (90%) for BMs of the face that were not biopsied but monitored over a period of more than 12 months without changing. Epidermal tumors, such as flat basal cell carcinomas and Bowen's diseases, were easily differentiated with this score from LM with an excellent specificity (93%). The early, ambiguous LMs were very often misclassified as BMs of the face under RCM. Indeed, it appeared that confocal and conventional light microscopy both have similar pitfalls when considering the shape of the cells and their organization with lesions that are of indeterminate malignancy.

In this series, we have acquired sufficient evidence to be confident that RCM can be used to help both the diagnosis of difficult macules of the face and to determine LM margins.

MATERIALS AND METHODS

Recruitment

Training set. Lesion recruitment was performed in two secondary care settings: the Sydney Melanoma Diagnostic Centre, Australia,

and the Department of Dermatology, University of Modena, Italy. Consecutive patients, presenting or found with a macule of the face and neck, which would be subjected to biopsy or excision to rule out an LM after conventional clinical and dermoscopy diagnosis, were entered into the study. The location had to be amenable to examination by RCM, as an adhesive ring of 2 cm must be used precluding the inclusion of lesion behind the ear, some parts of the edge of the nose or eyes. The recruitment criteria were the same at both the centers.

First, the study group included consecutive cases defined as:

1. A positive group in which the classical histological criteria of LM were present.
2. *Control groups*: macules of the face biopsied and not malignant (comprising solar-damaged skin, actinic keratoses, solar lentigo, lichen planus-like keratoses, seborrheic keratoses, ephelis, and junctional nevi).

When the lesion was not completely excised, aiming to obtain an accurate presurgical diagnosis or to assess the margins of very ill-defined tumors, 2–3 mm punch biopsies were performed in the center and then multiple biopsies in the margins of the lesion were conducted. For margin determination, confocal images were obtained and corresponding 2 mm punch biopsies taken in a radial direction from the lesion edge until no evidence of LM was seen. The punch biopsy was targeted in the middle of the $4 \times 4\,mm^2$ confocal field of view. This method of biopsy targeting should allow a better histological–confocal sample correlation, in particular, for LM which often contains irregular margins of scattered cells that may give rise to sample issues during histological step sectioning.

Test set. The test set recruitment was different from the training set. It comprised 73 cases recruited at the above-mentioned two centers and at the Skin and Cancer Associates in Plantation, Florida, USA (Modena $n=9$, Florida $n=25$, and Sydney $n=39$ cases). It is noteworthy that although the Florida cases were imaged using the same RCM instrument, the RCM image recording was different from the other two centers, with lesser images archived. Nevertheless, all Florida cases were recruited with a minimum of one archived block and sufficient capture images to see the superficial epidermis, dermoepidermal junction, and papillary dermis. They were not consecutive cases nor taken from the determination of LM margins.

A second test set comprised 6 invasive LM melanomas, 13 epithelial tumors such as macular BCCs, and 9 LMs defined as early stage or equivocal by the pathologist. In addition, 30 macules of the face that had not been biopsied but followed up for more than 12 months with sequential digital dermoscopy imaging and have remained unchanged were also tested.

This study was approved by the Ethics Committees in Sydney (protocol number X05-0218) and in Modena (protocol number 1338/CE) and signed consent was obtained. All clinical investigations were conducted according to the Declaration of Helsinki Principles.

Instruments and acquisition procedure

Before biopsy, RCM images were acquired using a near-infrared reflectance confocal laser scanning microscope (Vivascope 1500, Lucid, Henrietta, NY), which uses an 830 nm laser beam with a maximum power of 35 mW. Instrument and acquisition procedures are described elsewhere (Rajadhyaksha *et al.*, 1999). Each image corresponds to a horizontal section at a selected depth with a $0.5 \times 0.5\,mm^2$ field of view, and a lateral resolution of 1.0 μm and axial resolution of 3–5 μm. A sequence of montage images (''block'' images) were acquired for each lesion at the level of the dermoepidermal junction to explore a $4 \times 4\,mm^2$ field of view per lesion. For large lesions, not completely comprised within the field of view, the device was centered on the lesion or on the portion with the most suspicious dermoscopic features and moved to several locations if the lesion was not homogenous. Confocal sections, beginning at the stratum corneum and ending inside the papillary dermis, were recorded in the middle and at areas of interest. More than 100 capture images per lesion were recorded.

RCM analysis

RCM features were described by two expert observers (GP and PG), blinded from anamnestic information, dermoscopy, and clinical aspects, but not for the location. In detail, each observer evaluated the images previously randomized, opening codified folders containing all the images acquired for the corresponding case. At the end of the study, the patients' codes were broken and the evaluations were matched with pathology before statistical analysis.

For the training set, a series of 64 features, corresponding to 37 previous observations (Pellacani *et al.*, 2007) and new descriptors were considered at 3 different depth levels. All these features were evaluated for the presence/absence (binary nonparametric data), with the exception of the number of pagetoid cells that were binarized for statistics according to the presence/absence of more than three pagetoid cells in five $0.5 \times 0.5\,mm^2$ images. Description and definitions are summarized in Table 1.

For the test set, only LM and RCM scores were calculated.

Dermoscopic images

1. In Modena, several images for each lesion were recorded using a digital videodermatoscope (FotoFinder, TeachScreen Software GmbH, Bad Birnbach, Germany) with 20-, 30-, and 50-fold magnification (Grana *et al.*, 2005).
2. In Sydney, dermoscopy images were recorded on the field of view of the confocal microscope using the attached digital videodermatoscope (Vivacam, Lucid), with 35-fold magnification .

The color of the lesion was established on dermoscopic images and classified into three morphological dermoscopic variants: (1) Amelanotic lesions have no melanin pigmentation (tan, dark brown, blue, gray, black) upon dermoscopy inspection. Tan pigmentation is defined as light-brown pigmentation darker than the surrounding skin. (2) Light-colored (slightly pigmented) lesions have only tan, light blue or light gray pigmentation, which may occupy $>25\%$ of its total surface area. No dark brown, deep blue, or black color is found. (3) Partially and totally pigmented: the remainder of the lesions.

Statistics

Statistical evaluation was carried out using the SPSS statistical package (release 12.0.0, 2003; SPSS, Chicago, IL) and the Stata

statistical software (release 10.0, Stata Corporation, College Station, TX; 2007).

Absolute and relative frequencies of the observations in benign and malignant lesions were obtained for each RCM feature. Significant differences between LMs and benign lesions were evaluated using the χ^2 test of independence (Fisher's exact test was applied if any expected cell value in the 2×2 table was <5). For an estimate of LM risk, a calculation of the OR and 95% confidence interval was carried out.

Multivariate discriminant analysis and binary logistic regression were performed for the identification of the independently significant features and for the validation of the efficacy of RCM in distinguishing between BM and LM. The study population was defined as LM. Logistic regression and discriminant analysis are useful for predicting the presence or absence of a characteristic or outcome based on values of a set of predictor variables, similar to linear regression model but suited to models in which the dependent variable is dichotomous. Stepwise forward selection was used to choose the features for the prediction model. Goodness-of-fit statistics and Wilk's lambda were used to determine whether the models adequately described the data for logistic regression and discriminant analysis, respectively. At each step, the predictor with the largest score statistic the significance value of which is less than the default value of 0.05 for logistic regression and the largest F to Enter value that exceeds the entry criteria (by default, 3.84) for discriminant analysis, were added to the models. Variables with score statistic value >0.05 and with F to Enter values smaller than 3.84 were left out the models. A coefficient is estimated for each included variable in relation to the likeliness to predict an LM. The leave-one-out method was used to evaluate the predictive performance of the classification rules step by step.

RCM features useful for the distinction between LM and BM were identified, and the individual criteria were scored according to the coefficient values estimated by discriminant analysis. A score of 1 or 2 was attributed to the variables with the coefficient value inferior or greater than 1, respectively. The attributed plus or minus sign was maintained for positive or negative predictors, respectively. This allowed the creation of a simple diagnostic method (suitable for clinical use) based on identification of major and minor RCM criteria for LM diagnosis. A total score was obtained for each lesion.

Sensitivity, specificity, diagnostic accuracy, OR, and 95% confidence interval, were calculated for each score value. Sensitivity, specificity, diagnostic accuracy, OR, and 95% confidence interval, of the simplified algorithm were also calculated for amelanotic-hypopigmented lesions, pigmented lesions, and lesions not included in the study populations, such as LM melanomas, epithelial tumors, monitored BMs, and ''early'' LMs.

Finally, 35 BMs of the face and 35 LMs within the training set were evaluated by both the observers to calculate the agreement for each feature. We computed the κ-statistics for evaluation of interobserved agreement, by calculating Cohen's κ-statistics measure for each descriptor.

A *P*-value <0.05 was considered significant.

CONFLICT OF INTEREST

The authors state no conflict of interest.

ACKNOWLEDGMENTS

We thank Dr Tony Bonin for the editing of this paper. This study was supported by a grant from the Istituto Superiore di Sanità (ISS), (project number 527/B/3A/4), Italy, and the Cancer Institute, NSW, Australia.

REFERENCES

Ackerman AB, Briggs PL, Bravo F (1993) *Differential Diagnosis in Dermopathology III*. Philadelphia: Lea&Febiger, 166–9

Agarwal-Antal N, Bowen GM, Gerwels JW (2002) Histologic evaluation of lentigo maligna with permanent sections: implications regarding current guidelines. *J Am Acad Dermatol* 47:743–8

Agero AL, Busam KJ, Benvenuto-Andrade C *et al.* (2006) Reflectance confocal microscopy of pigmented basal cell carcinoma. *J Am Acad Dermatol* 54:638–43

Bene N, Healy C, Coldiron BM (2008) Mohs micrographic surgery is accurate 95.1% of the time for melanoma *in situ*: a propective study of 167 cases. *Dermatol Surg* 34:660–4

Barlow JO, Maize J Sr, Lang PG (2007) The density and distribution of melanocytes adjacent to melanoma and nonmelanoma skin cancers. *Dermatol Surg* 33:199–207

Barlow RJ, White CR, Swanson NA (2002) Mohs' micrographic surgery using frozen sections alone may be unsuitable for detecting single atypical melanocytes at the margins of melanoma *in situ*. *Br J Dermatol* 146:290–4

Bhardwaj SS, Tope WD, Lee PK (2006) Mohs micrographic surgery for lentigo maligna and lentigo maligna melanoma using Mel-5 immunostaining: University of Minnesota experience. *Dermatol Surg* 32:690–6

Bricca GM, Brodland DG, Ren D *et al.* (2005) Cutaneous head and neck melanoma treated with Mohs micrographic surgery. *J Am Acad Dermatol* 52:92–100

Bub JL, Berg D, Slee A *et al.* (2004) Management of lentigo maligna and lentigo maligna melanoma with staged excision: a 5-year follow-up. *Arch Dermatol* 140:552–8

Chen CS, Elias M, Busam K *et al.* (2005) Multimodal *in vivo* optical imaging, including confocal microscopy, facilitates presurgical margin mapping for clinically complex lentigo maligna melanoma. *Br J Dermatol* 153:1031–6

Cohen LM (1996) The starburst giant cell is useful for distinguishing lentigo maligna from photodamaged skin. *J Am Acad Dermatol* 35:962–8

Curiel-Lewandrowski C, Williams CM, Swindells KJ *et al.* (2004) Use of *in vivo* confocal microscopy in malignant melanoma: an aid in diagnosis and assessment of surgical and nonsurgical therapeutic approaches. *Arch Dermatol* 140:1127–32

Dalton SR, Gardner TL, Libow LF *et al.* (2005) Contiguous lesions in lentigo maligna. *J Am Acad Dermatol* 52:859–62

Erlandson RA (1987) Ultrastructural diagnosis of amelanotic malignant melanoma: aberrant melanosomes, myelin figures or lysosomes? *Ultrastruct Pathol* 11:191–208

Ferrara G, Zalaudek I, Argenziano G (2008) Lentiginous melanoma: a distinctive clinicopathological entity. *Histopathology* 52:523–5

Gibson LE, Goellner JR (1988) Amelanotic melanoma: cases studied by Fontana stain, S-100 immunostain, and ultrastructural examination. *Mayo Clin Proc* 63:777–82

Grana C, Pellacani G, Seidenari S (2005) Practical color calibration for dermoscopy, applied to a digital epiluminescence microscope. *Skin Res Technol* 11:242–7

Guitera P, Pellacani G, Longo C *et al.* (2009) *In vivo* reflectance confocal microscopy enhances secondary evaluation of melanocytic lesions. *J Invest Dermatol* 129:131–8

Hazan C, Dusza SW, Delgado R *et al.* (2008) Staged excision for lentigo maligna and lentigo maligna melanoma: a retrospective analysis of 117 cases. *J Am Acad Dermatol* 58:142–8

Huilgol SC, Selva D, Chen C *et al.* (2004) Surgical margins for lentigo maligna and lentigo maligna melanoma: the technique of mapped serial excision. *Arch Dermatol* 140:1087–92

Jeneby TT, Chang B, Bucky LP (2001) Ultraviolet-assisted punch biopsy mapping for lentigo maligna melanoma. *Ann Plast Surg* 46:495–9

Klauder JV, Beerman H (1955) Melanotic freckle (Hutchinson), mélanose circonscrite précancéreuse (Dubreuilh). *AMA Arch Derm* 71:2–10

Kossard S, Commens C, Symons M *et al.* (1991) Lentinginous dysplastic naevi in the elderly: a potential precursor for malignant melanoma. *Australas J Dermatol* 32:27–37

Langley RG, Burton E, Walsh N *et al.* (2006) *In vivo* confocal scanning laser microscopy of benign lentigines: comparison to conventional histology and *in vivo* characteristics of lentigo maligna. *J Am Acad Dermatol* 55:88–97

Mahoney MH, Joseph M, Temple CL (2005) The perimeter technique for lentigo maligna: an alternative to Mohs micrographic surgery. *J Surg Oncol* 91:120–5

McKenna JK, Florell SR, Goldman GD *et al.* (2006) Lentigo maligna/lentigo maligna melanoma: current state of diagnosis and treatment. *Dermatol Surg* 32:493–504

Moehrle M, Dietz K, Garbe C *et al.* (2006) Conventional histology versus three-dimensional histology in lentigo maligna melanoma. *Br J Dermatol* 154:453–9

Nori S, Rius-Díaz F, Cuevas J *et al.* (2004) Sensitivity and specificity of reflectance-mode confocal microscopy for *in vivo* diagnosis of basal cell carcinoma: a multicenter study. *J Am Acad Dermatol* 51:923–30

Osborne JE, Hutchinson PE (2002) A follow-up study to investigate the efficacy of initial treatment of lentigo maligna with surgical excision. *Br J Plast Surg* 55:611–5

Pellacani G, Guitera P, Longo C *et al.* (2007) The impact of *in vivo* reflectance confocal microscopy for the diagnostic accuracy of melanoma and equivocal melanocytic lesions. *J Invest Dermatol* 127:2759–65

Rajadhyaksha M, Gonzalez S, Zavislan JM *et al.* (1999) *In vivo* confocal scanning laser microscopy of human skin II: advances in instrumentation and comparison with histology. *J Invest Dermatol* 113:293–303

Rajadhyaksha M, Grossman M, Esterowitz D *et al.* (1995) *In vivo* confocal scanning laser microscopy of human skin: melanin provides strong contrast. *J Invest Dermatol* 104:946–52

Robinson JK (2004) Use of digital epiluminescence microscopy to help define the edge of lentigo maligna. *Arch Dermatol* 140:1095–100

Schiffner R, Schiffner-Rohe J, Vogt T *et al.* (2000) Improvement of early recognition of lentigo maligna using dermatoscopy. *J Am Acad Dermatol* 42:25–32

Stante M, Giorgi V, Stanganelli I *et al.* (2005) Dermoscopy for early detection of facial lentigo maligna. *Br J Dermatol* 152:361–4

Tannous ZS, Mihm MC, Flotte TJ *et al.* (2002) *In vivo* examination of lentigo maligna and malignant melanoma *in situ*, lentigo maligna type by near-infrared reflectance confocal microscopy: comparison of *in vivo* confocal images with histologic sections. *J Am Acad Dermatol* 46:260–3

Weyers W, Bonczkowitz M, Weyers I *et al.* (1996) Melanoma *in situ* versus melanocytic hyperplasia in sun-damaged skin. Assessment of the significance of histopathologic criteria for differential diagnosis. *Am J Dermatopathol* 18:560–6

Zitelli JA, Moy RL, Abell E (1991) The reliability of frozen sections in the evaluation of surgical margins of melanoma. *J Am Acad Dermatol* 24:102–6